Available online at www.sciencedirect.com

ScienceDirect

journal homepage: www.elsevier.com/locate/he

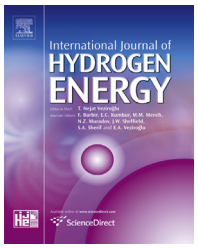

Experimental and modeling study of hydrogen production from catalytic steam reforming of methane mixture with hydrogen sulfide

Parham Sadooghi [a,*], *Reinhard Rauch* [b]

[a] *Vienna University of Technology, Vienna, Austria*
[b] *Bioenergy 2020+ GmbH, Güssing, Austria*

ARTICLE INFO

Article history:
Received 20 March 2015
Received in revised form
19 June 2015
Accepted 28 June 2015
Available online 21 July 2015

Keywords:
Methane
Sulfur
Catalysis
Reforming
Heat
Reactor

ABSTRACT

Experimental and theoretical studies of steam methane reforming reactions with different amount of hydrogen sulfide in the feed gas are presented. A two dimensional pseudo-heterogeneous model is developed to simulate methane steam reforming reactions in a packed bed tubular reactor. This model is based on mole and energy balance equations for the catalyst and the fluid phases. Attention is given to the analysis of sulfur negative effects on reforming process. A parametric study is done and effects of different steam to carbon ratios, space velocities, temperatures and different amount of sulfur on methane conversion and temperature distribution within the reactor are investigated. The results are verified comparing to the experimental results. It is shown that even presented in the gas at very low concentration levels (ppm), sulfur drastically decreases the conversion of methane. The obtained results play a key role in design and optimization of an actual reactor.
Copyright © 2015, Hydrogen Energy Publications, LLC. Published by Elsevier Ltd. All rights reserved.

Introduction

In the latest years, the environmental problems derived from useful energy generation sources and from the increment of fossil fuels prices, have enhanced the development of new technologies for energy production. Steam reforming of methane produced by biomass gasification is one of the most employed processes to produce hydrogen and synthesis gas [1–4]. Synthesis gas, constituted by different quantities of carbon monoxide and hydrogen, can also be used to produce high purity hydrogen streams and chemical products, [5]. The steam reforming reactions are industrially operated at a high temperature up to 900 °C over nickel-alumina or noble metal based catalysts, because a reasonable conversion of methane is required in this endothermic process, [6–8]. Sulfur, on the other hand, which also is incorporated in the biomass structure, is released into the product gas during gasification as hydrogen sulfide. It is generally recognized that sulfur can have devastating effects on the catalytic activity of supported metal particles. Many catalytic reactions are poisoned by even trace quantities of sulfur containing molecules such as hydrogen sulfide. Since, synthesis gas produced by steam reforming of low hydrocarbons are further used in the

* *Corresponding author*. Tel.: +43 1 58801 0; fax: +43 1 58801 41099.
E-mail address: parham.sadooghi@tuwien.ac.at (P. Sadooghi).
http://dx.doi.org/10.1016/j.ijhydene.2015.06.143
0360-3199/Copyright © 2015, Hydrogen Energy Publications, LLC. Published by Elsevier Ltd. All rights reserved.

synthesis to mixed alcohols or Fischer–Tropsch products, it is of interest to investigate steam reforming process without cleaning the gas and desulfurization prior to the reactor.

Even though, different methods have been used to address and simulate the steady state and non-steady state operation of catalytic steam reformers, and several comprehensive reviews have been written about reforming of methane [9–21], there is no mechanism available which covers steam reforming of methane including sulfur and published papers are very few in numbers, [22–30]. This work considers a two dimensional pseudo-heterogeneous model to mathematically simulate steam reforming of methane in a fixed bed reactor including reasonable amount of hydrogen sulfide. Using the same inlet and process condition for experiments, makes it possible to compare the modeling and experimental results and see how well the modeling predict the experimental results. Moreover, a parametric study is done to investigate the effects of different reforming parameters such as sulfur, space velocity, steam to carbon ratio and temperature on process efficiency.

Mathematical model

Steam reforming of methane involves, two reversible endothermic reforming reactions, (1, 3) coupled with exothermic water gas shift reaction, (2) [31],:

$$CH_4 + H_2O \leftrightarrow CO + 3H_2 \quad \Delta H^0_{298} = +206\text{kJ/mol} \tag{1}$$

$$CO + H_2O \leftrightarrow CO_2 + H_2 \quad \Delta H^0_{298} = -41\text{kJ/mol} \tag{2}$$

$$CH_4 + 2H_2O \leftrightarrow CO_2 + 4H_2 \quad \Delta H^0_{298} = +165\text{kJ/mol} \tag{3}$$

The kinetic model for methane steam reforming reactions on a nickel catalyst is based on a Langmuir–Hinshelwood reaction mechanism and the intrinsic kinetic expressions reported by Xu and Froment are adopted [10,11],:

$$R_1 = \frac{\frac{k_1}{P_{H_2}^{2.5}}\left[P_{CH_4}P_{H_2O} - \frac{P_{H_2}^3 P_{CO}}{K_1}\right]}{DEN^2} \tag{4a}$$

$$R_2 = \frac{\frac{k_2}{P_{H_2}}\left[P_{CO}P_{H_2O} - \frac{P_{H_2}P_{CO_2}}{K_2}\right]}{DEN^2} \tag{4b}$$

$$R_3 = \frac{\frac{k_3}{P_{H_2}^{3.5}}\left[P_{CH_4}P_{H_2O}^2 - \frac{P_{H_2}^4 P_{CO_2}}{K_3}\right]}{DEN^2} \tag{4c}$$

$$DEN = 1 + K_{CH_4}P_{CH_4} + K_{CO}P_{CO} + K_{H_2}P_{H_2} + \frac{K_{H_2O}P_{H_2O}}{P_{H_2}} \tag{4d}$$

Rate constants of the above equations are described by Arrhenius type functions [31],:

$$k_1 = 9.49 \times 10^{16} \exp\left(-\frac{28,879}{T}\right) \frac{\text{kmol kpa}^{0.5}}{\text{kg h}} \tag{5a}$$

$$k_2 = 4.39 \times 10^{4} \exp\left(-\frac{8074.3}{T}\right) \frac{\text{kmol kpa}}{\text{kg h}} \tag{5b}$$

$$k_3 = 2.29 \times 10^{16} \exp\left(-\frac{29,336}{T}\right) \frac{\text{kmol kpa}^{0.5}}{\text{kg h}} \tag{5c}$$

$K_{CH_4}, K_{H_2}, K_{CO}, K_{H_2O}$ are the constants which related to surface adsorption in equilibrium and are functions of temperature. The equilibrium constants for reactions (1–3) were calculated using the standard Gibbs energy of each reaction at the corresponding temperature and are defined as [31],:

$$K_1 = 10266.76 \times \exp\left(-\frac{26,830}{T} + 30.11\right); \text{kpa}^2 \tag{5d}$$

$$K_2 = \exp\left(\frac{4400}{T} - 4.063\right) \tag{5e}$$

$$K_3 = K_1K_2; \text{kpa}^2 \tag{5f}$$

Partial pressures of gases were correlated to their own concentrations by using the ideal gas law. The formation rate of each component was then calculated by using equations (1)–(5f). For example, for methane and carbon dioxide components the reaction rates are written as follow:

$$R_{CH_4} = -(R_1 + R_3) \tag{6a}$$

$$R_{CO_2} = (R_2 + R_3) \tag{6b}$$

Pseudo-heterogeneous model considers transport by plug flow and distinguishes between conditions in the fluid and in the solid (catalyst) phases. The continuity and energy balance equations for the fluid phase are written as [31],:

$$u_z\left(\frac{\partial C_i}{\partial z} + u_r\frac{\partial C_i}{\partial r}\right) = \frac{1}{r}\frac{\partial}{\partial r}\left(rD_{er}\frac{\partial C_i}{\partial r}\right) + k_g a_v\left(C_S^s - C_i\right) \tag{7a}$$

$$\frac{\partial T}{\partial z} = \frac{I}{\rho_f C_p u_z}\left(\lambda_{er}\left(\frac{1}{r}\frac{\partial T}{\partial r} + \frac{\partial^2 T}{\partial r^2}\right) - h_f a_v\left(T - T_s^s\right)\right) \tag{7b}$$

Where, a_v is the specific surface area of the catalyst bulk per reactor volume. The energy transport in axial direction is dominated by the transport from axial convection, and thus axial conduction is neglected. With no radial convection, the only energy transport mechanism in radial direction is the effective conduction.

When resistance to heat and mass transfer inside catalyst pellets is important, the rate of reaction is not uniform throughout the particle. The catalyst phase mass and energy balance equations are written as [31],:

$$k_g a_v(C^sS - C_i) = \rho_c(1-\varepsilon)\eta_i R_i \tag{8a}$$

$$h_p a_v\left(T_s^s - T_f\right) = \frac{1}{r}\frac{\partial}{\partial r}\left(r\lambda_{er}{}^s\frac{\partial T_s}{\partial r}\right) + \rho_c(1-\varepsilon)\sum(\eta_i(-\Delta H_i)R_i \tag{8b}$$

Momentum equation which shows the pressure distribution in the packed-bed reactor was described by the Tallmadge, who proposed an extension of Ergun's equation under higher Reynolds numbers [32,33],:

$$\frac{dp}{dz} = -\frac{f\rho_f {u_z}^2}{dp} \tag{9a}$$

$$f = \mu^2(\mu - 1)\left[1.75 + \frac{4.2(\mu-1)}{\mu \text{Re}_p{}^{1/6}}\right] \tag{9b}$$

The following general boundary and initial conditions are applied to the reformer [31],:

$$\text{at} \quad \begin{matrix} z = 0 \\ 0 \le r \le R \end{matrix} \rightarrow \begin{matrix} C_i = C_0 \\ T_f = T_S = T_0 \end{matrix} \tag{10a}$$

$$\text{at} \quad r = 0 \rightarrow \frac{\partial C_i}{\partial r} = \frac{\partial C_s}{\partial r} = 0 \tag{10b}$$

$$\text{at} \quad r = 0 \rightarrow \frac{\partial T_f}{\partial r} = \frac{\partial T_S}{\partial r} = 0 \tag{10c}$$

$$\text{at} \quad r = R \rightarrow \begin{matrix} \frac{\partial C_i}{\partial r} = \frac{\partial C_s}{\partial r} = 0 \\ T_f = T_s = T_w \end{matrix} \tag{10d}$$

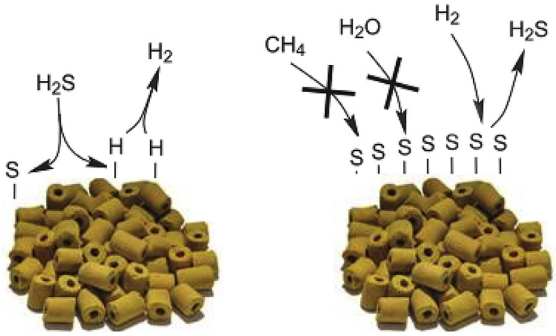

Fig. 1 – Sulfur poisoning scheme of the nickel catalysts.

$$\text{at} \quad r = r_p \rightarrow C_i = C_s^s \tag{10e}$$

$$\text{at} \quad r = r_p \rightarrow T = T_s^s \tag{10f}$$

Where C^s, T^s indicate the conditions at the surface of the catalyst. The effectiveness factor in the above reactions, which expresses the ratio of the observed rate to that calculated for surface conditions, are calculated as follows [32],:

$$\eta_i = \frac{\int_0^V r_i\left(p_j\right)\frac{dV}{V}}{r_i\left(p_j^s\right)} \quad i = 1, 2, 3 \tag{11}$$

The set of equations are solved simultaneously with pressure drop equation by state of the art COMSOL Multiphysics software 4.3, to account for species concentration and temperature distribution within the reactor. Wall heat transfer coefficient and thermal conductivity are calculated using the correlation reported by Dixon, [34,35].

Sulfur effects

Prior to steam reforming, sulfurous compounds must be removed from the feed stream because of their poisonous effects on the catalysts used. Under gasification and reforming conditions, all sulfur compounds in biomass will be converted to hydrogen sulfide, which is chemisorbed on the nickel surface and decreases the catalyst activity. Sulfur poisoning occurs because sulfur adsorbs strongly on the active metal surface area of the catalyst, forming surface sulfides. Sulfur is a selective poison and a

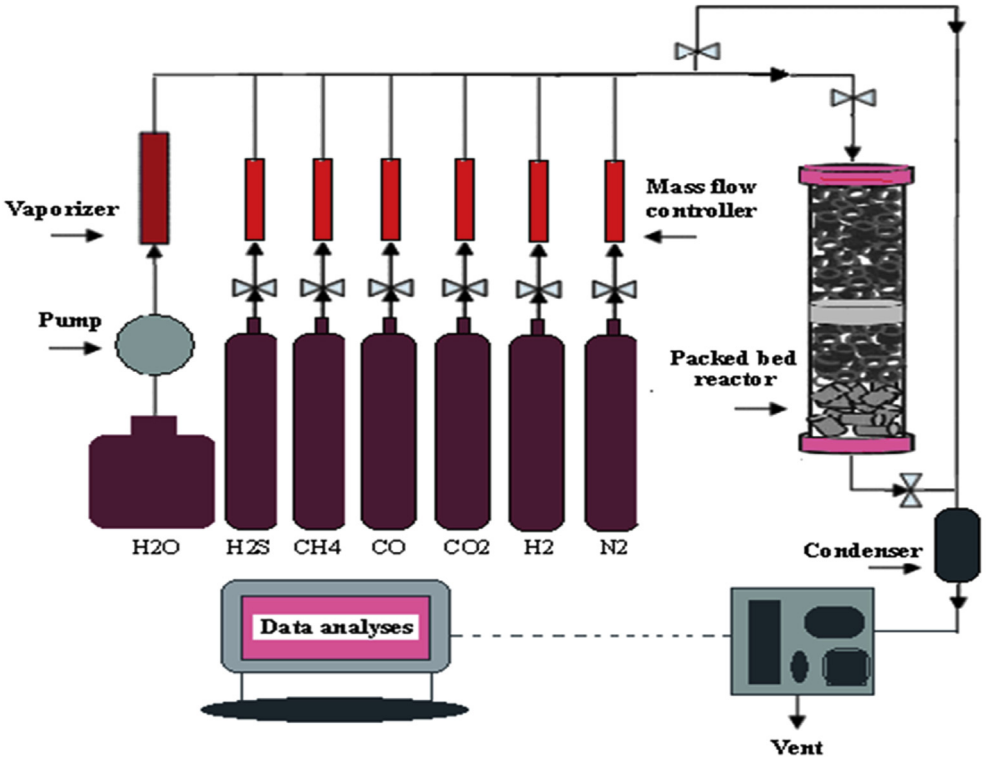

Fig. 2 – Schematic diagram of experimental setup.

Table 1 – Catalyst parameters and operating conditions.

Parameter	Value
Outside diameter of the catalyst	3.5 (mm)
Inside diameter of the catalyst	1.5 (mm)
Height of the catalyst particle	4 (mm)
Inlet pressure	1.163 (bar)
Inlet methane dry molar fraction	11 (%)
Inlet hydrogen dry molar fraction	39 (%)
Inlet carbon dioxide dry molar fraction	26 (%)
Inlet carbon monoxide dry molar fraction	22 (%)
Inlet nitrogen dry molar fraction	2 (%)
Catalyst bulk density	500 (kg/m^3)
Inside diameter of the reactor	16 (mm)
Height of the catalyst in the reactor	100 (mm)

partial surface coverage is sufficient for the catalyst to become essentially non-active which leads to the point that hydrocarbon conversion stops or is no longer at acceptable levels. This mechanism is shown in Fig. 1. Using a simple Maxted model for poisoning and Temkin isotherm, we recently compared the intrinsic rate expressions of poisoned catalyst to sulfur free catalyst, and modeled sulfur coverage, θ_s [27],:

$$R^s{}_i = R^{s0}{}_i(1-\theta_s)^3$$

$$\theta_s = 1.45 - 9.53\cdot10^{-5}\cdot T + 4.17\cdot10^{-5}\cdot T \ln\left(\frac{p_{H_2S}}{p_{H_2}}\right)$$

Rate expressions for sulfur free catalyst ($R^0{}_{sp}$), were discussed in previous sections.

Experimental procedure

The catalyst used in these experiments is a nickel based catalysts supported on alumina, ($NiAl_2O_3$). It is a cylinder shape catalyst with center hole. It has a constant outside diameter of 3.5 mm and inside diameter of 1.5 mm. The gases used in this study were chemically completely pure. The gas flow rate system consists of mass flow controllers which provide inlet gas in various blends of different gases, hydrogen, methane, carbon monoxide, carbon dioxide and Nitrogen as carrier gas. A bypass was inserted around the reactor allowing sampling of feed gas. Water is evaporated through heating tubes and a high performance liquid pump is used to control the liquid water flow rate. The liquid water was vaporized and mixed with the feed gas stream before entering the reactor. The reactor is made from a glass tube with 16 mm inside diameter. For the laboratory experiments typically 11 gr of catalyst was loaded into the reactor and the height of the catalyst bed is about 10 cm. The bulk density of the catalyst is 500 (kg/m^3). Due to endothermic nature of the process, heat should be supplied into the reactor; therefore, outer surface temperature of the reformer is kept at 1123 (K) by means of electrical heating. Thermocouples are placed within the reactor and are connected to a temperature indicator, computer monitoring system and temperature controllers. The gas leaving the reactor column was cooled in a condenser where liquid water is removed. Finally, the dry gas stream were routed into the online analyzer where their concentrations are analyzed, measured and presented in Lab view program which controls the online analyzer. A schematic diagram of experimental setup is shown in Fig. 2. Inlet gas conditions at different steam to carbon ratios, space velocities, sulfur concentrations and temperatures (depending on each experiment) were conducted in the reactor. The gases from the outlet of mass flow controllers are directed to come exactly above the packed bed and nitrogen is used as carrier gas. Different amount of water is fed into the reactor in order to adjust the desired steam to carbon ratio. Catalyst properties and operating conditions for the steam reformer are shown in Table 1.

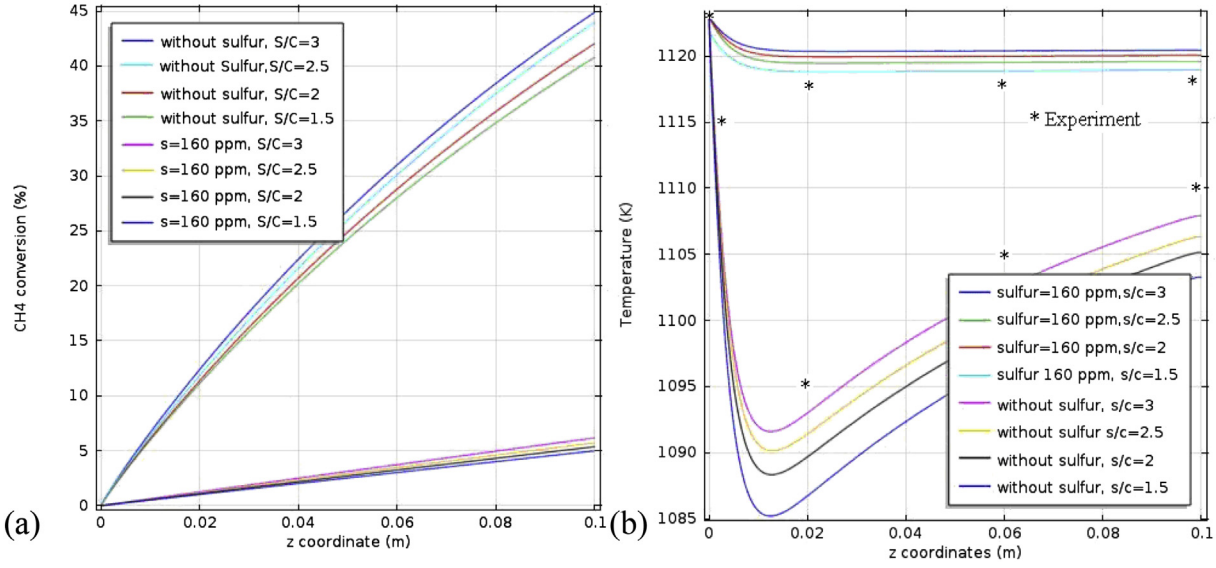

Fig. 3 – (a, b) Methane conversion and temperature distribution in the reactor, (a) methane conversion (b) axial temperature distribution.

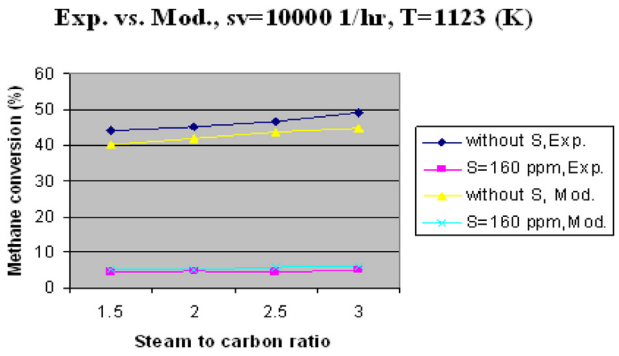

Fig. 4 – Comparison of modeling and experimental results of methane conversion.

Result and discussions

Modeling and experimental results presented in this work, provide the temperature distribution and methane conversion profiles along the reactor. Effects of different operating parameters such as steam to carbon ratio, different amount of sulfur, temperature distribution and space velocity on process efficiency are discussed in following sections.

Steam to carbon ratio effects

The effect of different steam to carbon ratios on methane conversion with and without sulfur included in the gas, are shown in Fig. 3(a). The reactor wall temperature is set at 1123 (K), the space velocity is 10,000 1/h. As it is shown by increasing steam to carbon ratio from 1.5 to 2.5, methane conversion increases significantly, but there is not a big difference in methane conversion when steam to carbon ratio increases from 2.5 to 3. Sulfur has huge negative effect on conversion process by deactivating the catalyst and methane conversion decreases drastically. The effect of different steam to carbon ratios on temperature distribution along the reactor is shown in Fig. 3(b). When sulfur is not included in the gas, the temperature decreases as soon as the gas enters the reactor and then increases. This is due to the high endothermic nature of the reforming reactions which decreases the temperature. Later, heat transfer from the outer surface of the reactor, increases the temperature again. Increasing the steam to carbon ratio increases the outlet temperature due to the exothermic nature of the water gas shift reaction. When sulfur is included in the gas, deactivates the catalyst and decreases the reaction rate of reforming reactions. Therefore, the temperature decreases uniformly up to the outlet of the reactor. In both cases, with and without sulfur, increasing steam to carbon ratio makes temperature distribution more uniform along the reactor length. Experimental results are compared to modeling results in Fig. 3(b) and Fig. 4 for temperature distribution and methane conversion respectively. Although experimental and modeling results are in very good agreement in both cases, with and without sulfur included in the gas, when sulfur is included in the gas, due to deactivation effects of sulfur on highly endothermic reforming reactions, modeling predicts the experimental results exactly.

Sulfur effects

The effect of different amount of sulfur on methane conversion and temperature distribution is investigated in Fig. 5(a,b) and Fig. 6. The reactor wall temperature is set at 1123 (K) and kept constant, the space velocity is 10,000 1/h and steam to carbon ratio is set at 3, (S/C = 3). As it is shown in Fig. 5(a), even at very low concentration levels of hydrogen

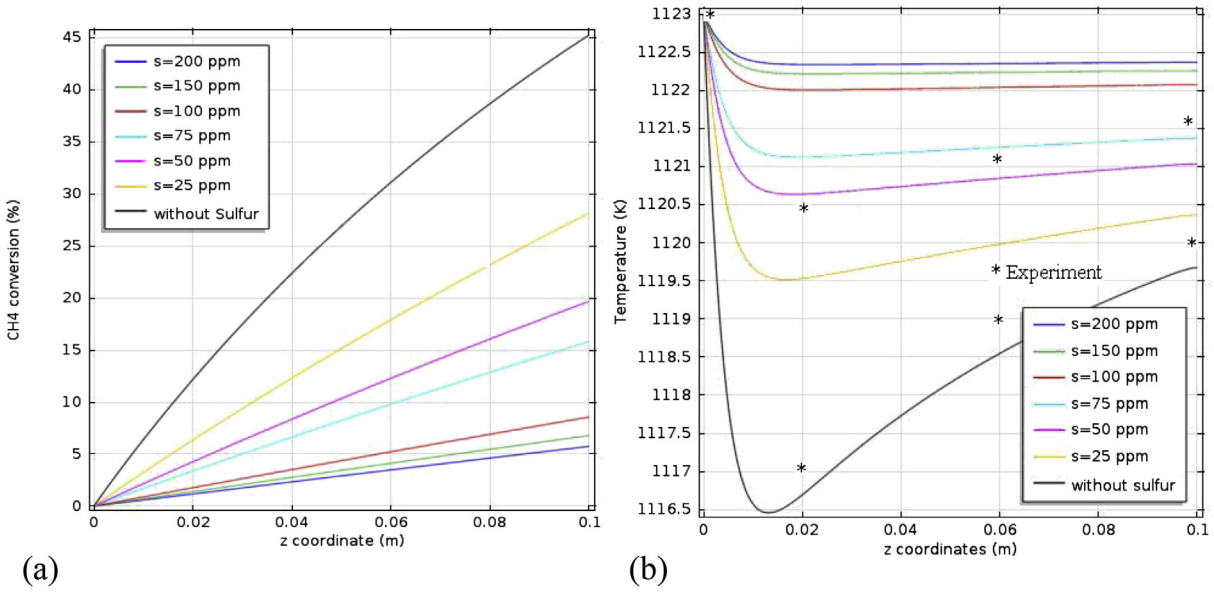

Fig. 5 – (a, b) Methane conversion and temperature distribution in the reactor, (a) methane conversion (b) axial temperature distribution.

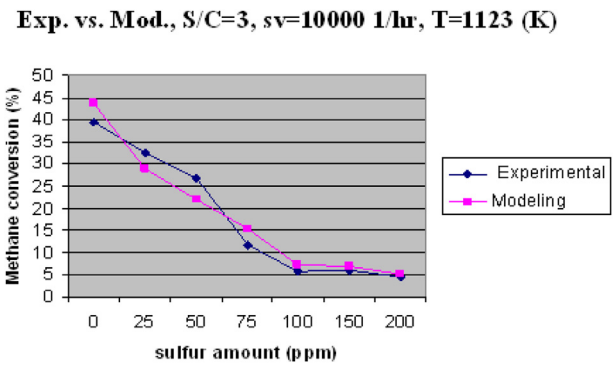

Fig. 6 – Comparison of modeling and experimental results of methane conversion in the reactor.

sulfide (25 ppm), catalytic activity is highly reduced and methane conversion is about 90 percent less than the case where there is no sulfur included in the gas. When hydrogen sulfide level increases to 150 ppm, it is shown that the catalyst is almost deactivated and increasing the concentration level does not decrease the methane conversion significantly.

Temperature distribution along the reactor is shown in Fig. 5(b). Hydrogen sulfide deactivates the catalyst and reforming reactions. As a result, temperature does not decrease significantly in the reactor. Heat transfer from the outer surface of the reactor increases the outlet temperature compare to the case when sulfur is not included in the gas. Increasing the hydrogen sulfide level of concentration, makes temperature distribution more uniform along the reactor. Experimental and modeling results of methane conversion are shown in Fig. 6. As it is mentioned in previous section, experimental and modeling results are in very good agreement at higher level of sulfur included in the gas.

Temperature effects

Fig. 7(a,b) and 8 show the effect of different temperatures on methane conversion and temperature distribution in the reactor. Space velocity is 10,000 1/h, steam to carbon ratio is set to 3 and sulfur amount is constant and is set to 160 ppm and the temperature varies from 1000 to 1150 (K). As it is shown in Fig. 7(a,b), increasing reactor wall temperature, heavily affects conversion of methane and temperature distribution in the reactor. Even when sulfur is included in the gas, increasing temperature, increases methane conversion significantly. Higher wall temperature also affects temperature distribution within the reactor by increasing the reaction rate of reforming reactions. Therefore, as it is shown in Fig. 7(b), when sulfur is not included in the gas, temperature decreases more significantly as soon as the gas enters the reactor. This is because of endothermic nature of the reforming reactions. Later, wall temperature supplies more heat into the reactor and increases the temperature along the reactor gradually. As it is shown, higher wall temperature increases the temperature at the outlet of the reactor. Comparison of experimental and modeling result of methane conversion at different temperatures are shown in Fig. 8. It shows very good agreement between simulation and experiment results.

Space velocity effects

Space velocity is an important parameter for design and optimization of steam reformers and has a high impact on methane conversion and temperature distribution within the reactor. In Fig. 9(a,b) and Fig. 10, it is shown that how changing space velocity affects the reformer performance. Steam to carbon ratio is set at 3, (S/C = 3) and sulfur amount is constant and is set to 160 ppm and outer reactor wall surface temperature is kept at 1123 (K). Fig. 9(a) shows the

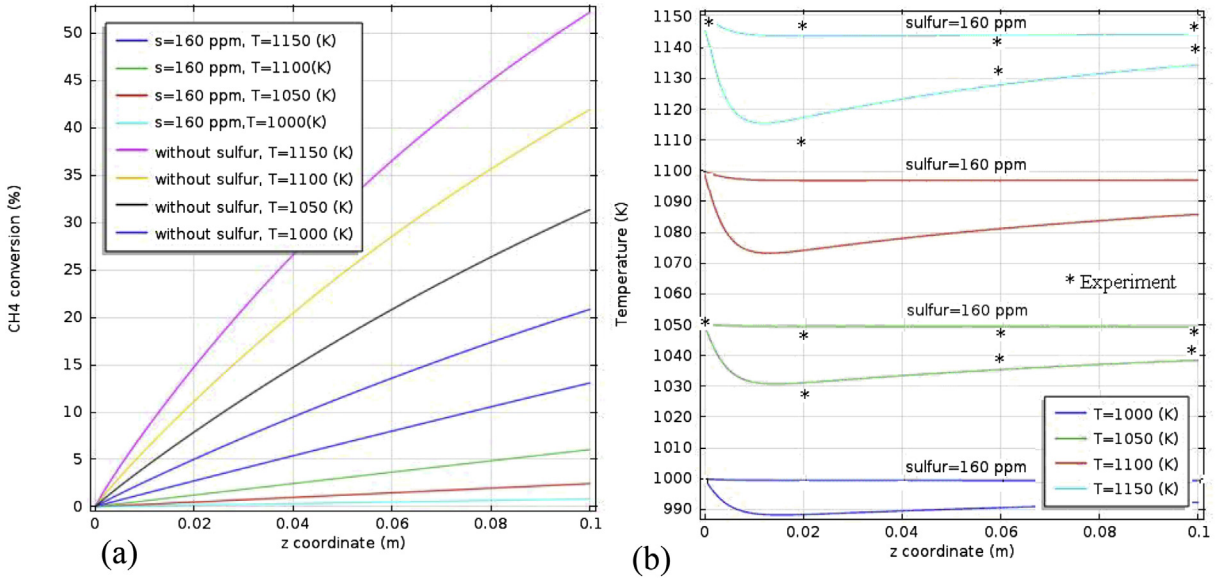

Fig. 7 – (a, b) Methane conversion and temperature distribution in the reactor, (a) methane conversion (b) axial temperature distribution.

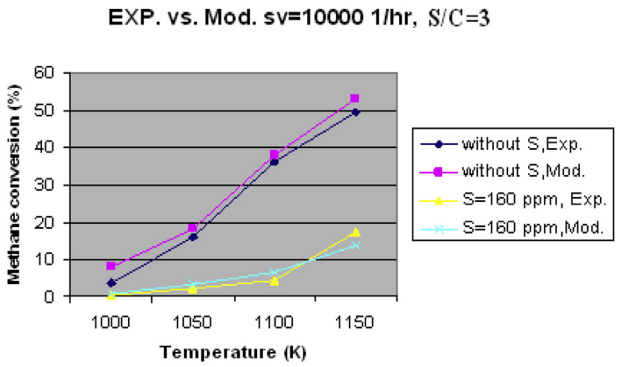

Fig. 8 – Comparison of modeling and experimental results of methane conversion in the reactor.

effect of different space velocities on methane conversion with and without presence of sulfur in the gas. It is evident that decreasing space velocity increases methane conversion. The reason is that at lower space velocities the contact time between gas and catalyst pellets increases and as a result methane conversion increases. When sulfur is included in the gas, the same effect is seen but methane conversion and therefore, hydrogen yield are decreased due to negative effect of sulfur on reforming reactions.

Temperature distribution along the reactor length is shown in Fig. 9(b). As it is seen, increasing space velocity does not affect temperature drop as soon as the gas enters the reactor. The reason is that reforming reactions take place very quickly and are not affected by changing space velocity at very short distance from the inlet. Decreasing space velocity increases heat transfer from the reactor wall to the gas and therefore increases the outlet temperature. Addition of sulfur to the gas makes temperature distribution more uniform within the reactor due to its deactivating effects on reforming reactions. Experimental and modeling results of methane conversion are compared in Fig. 10. It shows that how well modeling predicts experimental results and when sulfur is included in the gas, the results are very exact.

Conclusion

Two-dimensional heterogeneous model is developed to investigate hydrogen sulfide deactivation effects on methane steam reforming process in a packed bed reactor. Producer gas from biomass gasification has small amounts of hydrogen sulfide which deactivates the catalyst under reforming conditions. The novelty of the work is that the effect of different amount of hydrogen sulfide on methane conversion and temperature distribution within the reactor under different processing conditions such as space velocity, temperature, and steam to carbon ratio are investigated. A wide range of experiments have been done and the simulation and experimental results are compared. It is shown that even when present in the gas in very small amount of concentration level (ppm) sulfur decreases the reforming efficiency drastically and has a huge effect on temperature distribution within the reactor. The obtained results from simulation are compared with experimental results. Although experimental and modeling results are in very good agreement in both cases, with and without sulfur included in the gas, when sulfur is included in the gas, due to deactivation effects of sulfur on highly endothermic reforming reactions, modeling predicts the experimental results almost exactly. It is shown that some of the sulfur negative effects can be reduced by increasing the temperature, at which the steam reforming is run.

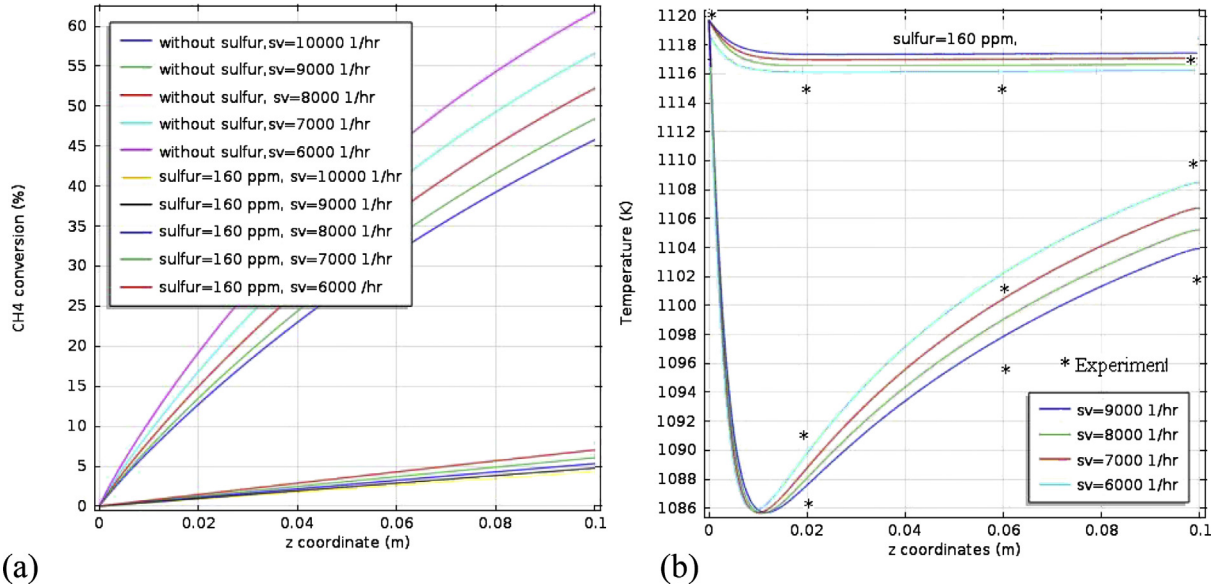

Fig. 9 – (a, b) Comparison of methane conversion and temperature distribution at different space velocities within the reactor with and without sulfur, S/C = 3, T = 1120 (K), (a) methane conversion, (b) axial temperature distribution.

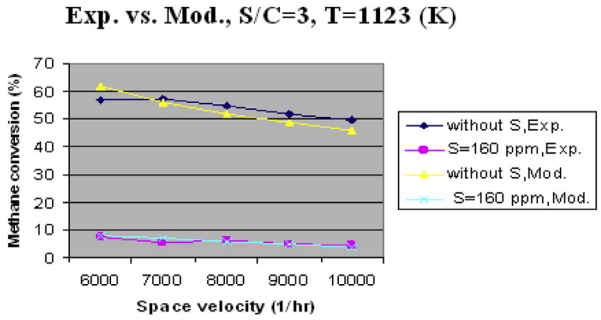

Fig. 10 – Comparison of modeling and experimental results of methane conversion in the reactor.

Acknowledgments

The authors wish to acknowledge the financial support of the Austrian Climate and Energy Fund since this work was carried out under the Projects ''distributed SNG'' and ''BioH2-4industries''. Moreover the authors acknowledge the financial support of the Austrian COMET program, where within the Bioenergy2020+ projects ''BioH2'' and "Mixed Alcohols" a part of the work was carried out.

Nomenclature

a_v	External pellet surface area per unit reactor volume m_p^2/m_r^3
C_i	Concentration of reactant ikmol/m^3
C_p	Specific heat capacity J/(Kg*K)
C_s	Solid concentration kmol/m^3
d_i	Inner diameter m
d_o	Outer diameter m
d_p	Equivalent particle diameter m
DEN	Denominator in the expressions of reaction rates
D_{er}	Effective radial diffusion coefficient m^2/s
f	Friction factor
h_f	Heat transfer coefficient at catalyst surface W/(m^{2}K)
k_g	Mass transfer coefficient from gas to solid interface $m_f^3/(m_i^2)$
K_j	Adsorption constant of component j
k_1	Rate coefficient of reaction 1 kmol bar$^{-0.5}$(kg cat s)
k_2	Rate coefficient of reaction 2 kmol/(kg cat bar s)
k_3	Rate coefficient of reaction 3 kmol bar$^{-0.5}$(kg cat s)
K_i	Equilibrium constant of reaction i
K_1	Equilibrium constant of reaction 1 bar^2
K_2	Equilibrium constant of reaction 2
K_3	Equilibrium constant of reaction 3 bar^2
n	Molar flow rate kmol/s
p	Pressure bar
P_i	Partial pressure of component i bar
R	Radius of the reactor m
R_g	Gas constant kJ/(kmol K)
Re_p	Particle Reynolds number
R_i	Reaction rate of component i mol/(kg cat s)
R_i^{S0}	Free sulfur reaction rate mol/(kg cat s)
R_i^S	Reaction rate with sulfur mol/(kg cat s)
R_j	Reaction rate of component j mol/(kg cat s)
R_1	Reaction rate of reaction 1 mol/(kg cat s)
R_2	Reaction rate of reaction 2 mol/(kg cat s)
R_3	Reaction rate of reaction 1 mol/(kg cat s)
R_4	Reaction rate of reaction 4 mol/(kg cat s)
T	Temperature K
T_w	Wall temperature K
u_r	Gas velocity in radial direction m/s
u_z	Gas velocity in axial direction m/s
V	Volume m^3

Greek letters

ΔH^0	Enthalpy of formation kJ/mol
ε	Porosity of packed bed reactor
η_i	Effectiveness factor of reaction i
λ_{er}	Effective thermal conductivity W/(mK)
μ	Viscosity of the mixture Pa s
ρ_f	Fluid density kg/m^3
ρ_c	Catalyst density kg/m^3
θ_s	Sulfur surface coverage

Subscripts

0	Initial condition
c	Catalyst
er	Effective
f	Fluid
g	Gas
p	Particle
r	Radial direction
S	Solid
w	Reactor wall
z	Axial direction

Superscripts

0	Standard condition
s	Condition at the catalyst surface

REFERENCES

[1] Crocker M. Thermo-chemical conversion of biomass to liquid fuels and chemicals. 1st ed. Royal Society of Chemistry; 2010.
[2] Feng W, Bo Q, Guoqiang W, Longjian L. Methane steam reforming: kinetics and modeling over coating catalyst in micro-channel reactor. Int J Hydrogen Energy 2013;38(14):5693–704.
[3] Brwon CR. Thermo-chemical processing of biomass conversion into fuels and power. 1st ed. Wiley; 2011.
[4] So Yun L, Hankwon L, Hee Chul W. Catalytic activity and characterizations of Ni/$K_2Ti_xO_y$–Al_2O_3 catalyst for steam methane reforming. Int J Hydrogen Energy 2014;39(31):17645–55.
[5] Sadooghi P, Rauch R. Pseudo heterogeneous modeling of catalytic methane steam reforming process in a fixed bed reactor. J Nat Gas Sci Eng 2013;11:46–51.
[6] Rostrup-Nielsen JR. Manufacture of hydrogen. Catal Today 2005;106:293–301.
[7] Shabbir A, Sheldon HDL, Magali SF. Catalytic steam reforming of biogas – effects of feed composition and operating conditions. Int J Hydrogen Energy 2015;40(2):1005–15.
[8] Sadooghi P, Rauch R. Experimental and modeling study of catalytic steam reforming of methane mixture with

propylene in a packed bed reactor. Int J Heat Mass Transf 2014;78:515–21.
[9] Xu J, Froment GF. Methane steam reforming: I, methanation and water-gas shift reaction, intrinsic kinetics. AIChE J 1989a;35(1):88–96.
[10] Xu J, Froment GF. Methane steam reforming: II, diffusional limitations and reactor simulation. AIChE J 1989b;35(1):97–103.
[11] Zanfir M, Gavriilidis A. Catalytic combustion assisted methane steam reforming. Chem Eng Sci 2003;58:3947–60.
[12] Therdthianwong A, Sakulkoakiet T, Therdthianwong S. Hydrogen production by catalytic ethanol steam reforming. Sci Asia 2001;27:193–9.
[13] Rostrup-Nielsen JR. Catalytic steam reforming. In: Anderson JR, Boudart M, editors. Catalysis: science and technology. Springer; 1984.
[14] Matsumura Y, Nakamori T. Steam reforming of methane over nickel catalysts at low reaction temperature. Appl Catal A 2004;258:107–14.
[15] Hou K, Hughes R. The kinetics of methane steam reforming over a nickel catalyst. Chem Eng J 2001;82:311–28.
[16] Rostrup-Nielsen JR, Hansen J. CO2 reforming of methane over transition metals. J Catal 1993;144:38–49.
[17] Rostrup-Nielsen JR, Sehested J, Nørskov J. Hydrogen and synthesis gas by steam and CO2 reforming. Adv Catal 2002;47:65–139.
[18] Trane-Restrup R, Dahl S, Jensen AD. Steam reforming of ethanol: effects of support and additives on Ni-based catalysts. Int J Hydrogen Energy 2013;38(35):15105–18.
[19] Liu K, Song C, Subramani V. Hydrogen and synthesis gas production and purification technologies. John Wiley & Sons; 2009.
[20] Grigorios P, Eustathios SK, Michael CG. A heterogeneous dynamic model for the simulation and optimisation of the steam methane reforming reactor,. Int J Hydrogen Energy 2012;37(21):16346–58.
[21] De Abreu J, Lucrédio A, Assaf E. Ni catalyst on mixed support of CeO_2 –ZrO_2 and Al_2O_3: effect of composition of CeO_2–ZrO_2 solid solution on the methane steam reforming reaction. Fuel Process Technol 2012;102:140–8.
[22] Alstrup I, Rostrup-Nielsen JR, Røen S. High temperature hydrogen sulfide chemisorption on nickel catalysts. Appl Catal 1981;1:303–14.
[23] Rostrup-Nielsen JR. Sulfur-passivated nickel catalysts for carbon-free steam reforming of methane. J Catal 1984;85:31–43.
[24] Fidalgo B, Muradov N, Menéndez JA. Effect of H_2S on carbon-catalyzed methane decomposition and CO_2 reforming reactions. Int J Hydrogen Energy 2012;37(19):14187–94.
[25] Christian H. Sulphur-tolerant catalysts in small-scale hydrogen production, a review. Int J Hydrogen Energy 2012;37(5):3978–92.
[26] Lakhapatri S, Abraham MA. Deactivation due to sulfur poisoning and carbon deposition on Rh-Ni/Al_2O_3 catalyst during steam reforming of sulfur-doped n-hexadecane. Appl Catal A Gen 2009;364(1–2):113–21.
[27] Sadooghi P, Rauch R. Mathematical modeling of sulfur deactivation effects on steam reforming of producer gas produced by biomass gasification. Fuel Process Technol 2013;110:46–52.
[28] Owens WT, Rodriguez NM, Baker RTK. Effect of sulfur on the interaction of nickel with ethylene. Catal Today 1994;21:3–22.
[29] Strohm J, Zehng J, Song C. Low temperature steam reforming of jet fuel in the absence and presence of sulfur over Rh and Rh–Ni catalysts for fuel cells. J Catal 2006;238(2):309–20.
[30] Wang L, Murata K, Inaba M. Development of novel highly active and sulphur-tolerant catalysts for steam reforming of liquid hydrocarbons to produce hydrogen. Appl Catal A Gen 2004;4:43–7.
[31] Froment GF, Bischoff BK, De Wilde J. Chemical reactor analysis and design. John Wiley & Sons; 2010.
[32] Ergun S. Fluid flow through packed columns. Chem Eng Prog 1952;48:89–94.
[33] Tallmadge JA. Packed bed pressure drop: an extension to higher Reynolds numbers. AIChE J 1970;19:1092–3.
[34] Dixon AG, DiCostanzo MA, Soucy BA. Fluid phase radial transport in packed beds. Int J Heat Mass Transf 1981;27:1701–13.
[35] Dixon AG, Cresswell DL. Theoretical prediction of effective heat transfer parameters in packed beds. AIChE J 1979;25:663–76.